European Journal of Pharmacology 746 (2015) 233–244

Contents lists available at ScienceDirect

European Journal of Pharmacology

journal homepage: www.elsevier.com/locate/ejphar

Molecular and cellular pharmacology

Cytotoxic and multidrug resistance reversal activities of novel 1,4-dihydropyridines against human cancer cells

Farnaz Shekari [a], Hossein Sadeghpour [b], Katayoun Javidnia [a], Luciano Saso [c], Farhad Nazari [a], Omidreza Firuzi [a,*], Ramin Miri [a,*]

[a] Medicinal and Natural Products Chemistry Research Center, Shiraz University of Medical Sciences, Shiraz, Iran
[b] Department of Medicinal Chemistry, Faculty of Pharmacy, Shiraz University of Medical Sciences, Shiraz, Iran
[c] Department of Physiology and Pharmacology "Vittorio Erspamer", Sapienza University of Rome, Rome, Italy

ARTICLE INFO

Article history:
Received 16 July 2014
Received in revised form
26 October 2014
Accepted 27 October 2014
Available online 14 November 2014

Keywords:
1,4-Dihydropyridine (CID 104822)
Multidrug resistance
Cytotoxicity
Rhodamine 123 (CID 65217)
P-glycoprotein

ABSTRACT

Multidrug resistance (MDR) caused by P-glycoprotein (P-gp, ABCB1, MDR-1) transporter over-expression in cancer cells substantially limits the effectiveness of chemotherapy. 1,4-Dihydropyridines (DHPs) derivatives possess several pharmacological activities. In this study, 18 novel asymmetrical DHPs bearing 3-pyridyl methyl carboxylate and alkyl carboxylate moieties at C_3 and C_5 positions, respectively, as well as nitrophenyl or hetero aromatic rings at C_4 were synthesized and tested for MDR reversal with the aim of establishing a structure–activity relationship (SAR) for these agents. Effect of these compounds on P-gp mediated MDR was assessed in P-gp over-expressing MES-SA/DX5 doxorubicin resistant cells by flow cytometric detection of rhodamine 123 efflux. MDR reversal was further examined as the alteration of doxorubicin's IC_{50} in MES-SA/DX5 cells in the presence of DHPs by MTT assay and was compared to nonresistant MES-SA cells. Direct anticancer effect was examined against 4 human cancer cells including HL-60, K562, MCF-7 and LS180. Calcium channel blocking (CCB) activity was also measured as a potential side effect. Most DHPs, particularly compounds bearing 3-nitrophenyl (A2B2 and A3B2) and 4-nitrophenyl (A3B1 and A4B1) moieties at C_4 significantly inhibited rhodamine 123 efflux at 5–25 μM, showing that the mechanism of MDR reversal by these agents is P-gp transporter modulation. Same derivatives were also able to selectively lower the resistance of MES-SA/DX5 to doxorubicin. A2B2 bearing ethyl carboxylate at C_5 had also high direct antitumoral effect (IC_{50} range: 3.77–15.60 μM). Our findings suggest that SAR studies of DHPs may lead to the discovery of novel MDR reversal agents.

1. Introduction

Multidrug resistance (MDR), defined as resistance of tumor cells to chemotherapeutic agents that are dissimilar in function and structure, is one of the main obstacles in conventional chemotherapy and an important cause of the failure of cancer treatment (Gottesman, 1993; Liscovitch and Lavie, 2002). MDR is linked with several different mechanisms. One important mechanism is over-expression of P-glycoprotein (P-gp), a protein encoded by the MDR-1 gene that belongs to ATP-binding cassette (ABC) membrane transporters family. MRP1, MRP2 and BCRP are other major ABC transporters associated with MDR (Ozben, 2006; Palmeira et al., 2012). P-gp pump mediates the efflux of different classes of chemotherapeutic drugs such as anthracycline derivatives, vinca alkaloids or podophyllotoxins. It has been shown that a variety of compounds with diverse structures are able to inhibit P-gp pump, one class of which are 1,4-dihydropyridines (1,4-DHPs) (Liu, 2009; Viale et al., 2011; Voigt et al., 2007).

1,4-DHPs are a useful class of calcium channel blocking (CCB) agents, commonly used for treatment of cardiovascular diseases (Sica, 2006; Yamakage and Namiki, 2002). DHPs have also shown a broad range of other pharmacological effects such as antioxidant, anticonvulsant, anti-inflammatory, antidiabetic and antitubercular properties (Edraki et al., 2009; Moghadam et al., 2006; Saini et al., 2008). MDR reversal has also been reported as one of the important pharmacological potentials of DHPs (Carosati et al., 2012; Zarrin et al., 2010). In 1980, Tsuruo et al. (1983) reported for the first time that DHPs demonstrated MDR reversal effects on cancer cell lines. It has been shown that the main mechanism of DHPs as MDR reversal agents is P-gp inhibition (Coburger et al., 2010; Edraki et al., 2009; Firuzi et al., 2013; Hilgeroth et al., 2013). However, detailed structure–activity relationship (SAR) studies of

Abbreviations: ABC, ATP-binding cassette; MDR, multidrug resistance; P-gp, P-glycoprotein; DHP, dihydropyridine; CCB, calcium channel blocking; MTT, thiazolyl blue tetrazolium bromide; Rh123, rhodamine 123.

* Corresponding authors. Tel.: +98 711 230 3872; fax: +98 711 233 2225.
E-mail addresses: firuzio@sums.ac.ir (O. Firuzi), mirir@sums.ac.ir (R. Miri).

http://dx.doi.org/10.1016/j.ejphar.2014.10.058
0014-2999/

these compounds are scares and they are much needed in order to establish the best structural features required for the MDR reversal effect.

On the other hand, several studies have shown intrinsic cytotoxicity of DHPs (Firuzi et al., 2013; Hahn et al., 1997; Sarkarzadeh et al., 2013), which appears to be stronger against tumor cell lines compared to non-cancer cells (Laupeze et al., 2001; Morshed et al., 2005).In continuation of our ongoing research programs focused on the design of potent MDR-reversal agents of DHP prototype (Firuzi et al., 2013; Foroughinia et al., 2008; Mehdipour et al., 2007), in this study, we synthesized novel asymmetrical 1,4-DHP derivatives containing 3-pyridyl methyl carboxylate at C_3, aromatic or hetero aromatic rings at C_4, and alkyl carboxylate at C_5 position and evaluated their inhibition of P-gp transporter and resultant MDR reversal activity on MES-SA/DX5 cell line using flow cytometry and MTT assays with the main aim of establishing a SAR for these compounds. Furthermore, cytotoxic activity evaluation of compounds was performed on four cancer cell lines including HL-60, K562, MCF-7 and LS180. When DHPs are designed for MDR reversal, their CCB activity could have important side effects on the cardiovascular system, hence *in vitro* CCB activity of synthesized compounds was also investigated to rule this effect as a potential adverse effect (Khoshneviszadeh et al., 2009).

2. Material and methods

2.1. Materials

Pyridine-3-yl-methanol, alkyl acetoacetate (alkyl: methyl, ethyl, isopropyl, t-butyl) and DMSO were purchased from Merck, Darmstadt, Germany. Rhodamine 123, thiazolyl blue tetrazolium bromide (MTT) and 2,2,6-trimethyl-4H-1,3-dioxin-4-one was from Sigma-Aldrich, Saint Louis, MO. RPMI 1640, Dulbecco's phosphate buffered saline 10 × and penicillin-G/streptomycin were products of Biosera, Ringmer, UK and FBS (Fetal Bovine serum) was from Invitrogen, San Diego, CA, USA. Doxorubicin and cisplatin were obtained from Ebewe Pharma, Unterach, Austria.

2.2. Chemistry

2.2.1. Synthesis of pyridin-3-yl-methyl-3-oxobutanoate (III)

A mixture of 20 mmol (3.86 g) of pyridine-3-yl-methanol **I** and 20 mmol (2.48 g) of 2,2,6-trimethyl-4H-1,3-dioxin-4-one **II** was refluxed in 10 ml xylene at 150 °C for 45 min. The formation of compound was confirmed by thin layer chromatography (TLC). After cooling the mixture, xylene was removed under reduced pressure and the product was purified by column chromatography over silica gel using petroleum ether–ethyl acetate (Yield: 83%).

IR (KBr): υ 2961(C–H aromatic), 1746 (CO, ester), 1715 (CO, ketone) cm^{-1}.

2.2.2. General synthesis of alkyl 3-aminocrotonate (A1–4)

A mixture of ammonium acetate (3 mmol) **IV** and alkylacetoacetate **a1–4** (2 mmol) were refluxed in 10 ml of corresponding alkyl alcohol derivative for 24 h. Afterwards the product was immediately used in subsequent reaction without further purification. The formation of product was confirmed by IR spectra.

Methyl 3-aminocrotonate (A1)

IR (KBr): 1716 (C=O, ester), 3511, 3333 (NH_2) cm^{-1}

Ethyl 3-aminocrotonate (A2)

IR (KBr): 1716 (C=O, ester), 3511, 3332 (NH_2) cm^{-1}

Isopropyl 3-aminocrotonate (A3)

IR (KBr): 1716 (C=O, ester), 3509, 3332 (NH_2) cm^{-1}

t-butyl 3-aminocrotonate (A4)

IR (KBr): 1717 (C=O, ester), 3450, 3336 (NH_2) cm^{-1}

2.2.3. General procedure for the synthesis of asymmetrical derivatives of 1,4-DHP (A1B1−A3B5)

A mixture of pyridin-3-yl-methyl-3-oxobutanoate **III**, alkyl 3-aminocrotonate **A1–4** and aryl or heteroaryl aldehydes **B1–5** was refluxed in 15 ml ethanol or isopropanol or t-butanol (corresponding to alkyl 3-aminocrotonate) overnight. The completion of the reaction was monitored using thin layer chromatography (TLC). After completion, the solvent was evaporated and the residue was purified by preparative TLC on silica gel using chloroform–ethanol (94−6) as mobile phase. The final product was recrystallized from diethyl ether or a mixture of diethyl ether/petroleum ether. Because of DHP derivatives sensitivity to light, all above procedures were carried out under a sodium lamp to prevent degradation of products by natural irradiation (Memarian and Mirjafari, 2005).

Melting points of synthetic compounds were determined on a hot stage apparatus (Electro thermal, Essex, UK) and are uncorrected. ^{1}H NMR spectra were performed by Burker-AdvanceDPX-500 MHz in d_1-chloroform and Tetramethylsilane (TMS) was used as the internal standard. Mass spectra were recorded on an Agilent spectrometer (Agilent technologies 9575c inert MSD, USA) and the IR spectra were obtained using a Perkin-Elmer spectrometer (KBr disk) (Perkin-Elmer, Waltham, MA).

2.2.3.1. 3-Pyridin-3-ylmethyl 5-methyl 2,6-dimethyl-4-(4-nitrophenyl)-1,4-dihydropyridine-3,5-dicarboxylate (A1B1). ^{1}H NMR (500 MHz, $CDCl_3$) δ_H (ppm): 2.35 and 2.37 (2s, 6H, C_2–CH_3 and C_6–CH_3), 3.63 (s, 3H, $COOCH_3$), 5.04 and 5.15 (dd, 2H, $COOCH_2$–pyridyl, J=12.60 Hz), 5.08 (s, 1H, DHP–C_4–H), 5.75 (brs, 1H, NH), 7.22–7.24 (m, 1H, pyridyl–H_5), 7.36(d, 2H, 4-nitro phenyl–$H_{2,6}$, J=8.75 Hz), 7.48 (d, 1H, pyridyl–H_4, J=7.85 Hz), 8.03 (d, 2H, *4-nitro* phenyl–$H_{3,5}$, J=8.75 Hz), 8.55 (s, 1H, pyridyl–H_2), 8.56 (d, 1H, pyridyl–H_6, J=3.5 Hz).

MS (EI), *m/z* (%): 423 (M^+, 8), 392 (4), 364 (4), 331 (11), 301 (100), 287 (10), 210 (10), 165 (18), 150 (9), 92(42).

IR (KBr): 3281 (NH), 3056 (CH-aromatic), 2927 (CH-aliphatic), 1702, 1676 (C=O), 1508, 1341 (NO_2) cm^{-1}.

2.2.3.2. 3-Pyridin-3-ylmethyl 5-ethyl 2,6-dimethyl-4-(4-nitrophenyl)-1,4-dihydropyridine-3,5-dicarboxylate (A2B1). ^{1}H NMR (500 MHz, $CDCl_3$) δ_H (ppm): 1.2 (*t*, 3H, $COOCH_2CH_3$, J=6.85 Hz), 2.35 and 2.37 (2s, 6H, C_2–CH_3 and C_6–CH_3), 4.08 (q, 2H, $COOCH_2CH_3$, J=6.85 Hz), 5.04 and 5.15 (dd, 2H, $COOCH_2$–pyridyl, J=12.55 Hz), 5.09 (s, 1H, DHP–C_4–H), 5.77 (brs, 1H, NH), 7.23–7.26 (m, 1H, pyridyl–H_5), 7.37 (d, 2H, 4-nitro phenyl–$H_{2,6}$, J=8.15 Hz), 7.48 (d, 1H, pyridyl–H_4), 8.03 (d, 2H, 4-nitro phenyl–$H_{3,5}$, J=8.15 Hz), 8.54 (m, 2H, pyridyl–$H_{2,6}$).

MS (EI), *m/z* (%): 437 (M^+, 5), 392 (3), 364 (4), 345 (6), 315 (100), 301 (4), 287 (4), 269 (4), 151 (5), 92 (21).

IR (KBr): 3297 (NH), 3084 (CH-aromatic), 2974 (CH-aliphatic), 1674 (C=O), 1516, 1348 (NO_2) cm^{-1}.

2.2.3.3. 3-Pyridin-3-ylmethyl 5-isopropyl 2,6-dimethyl-4-(4-nitrophenyl)-1,4-dihydropyridine-3,5-dicarboxylate (A3B1). ^{1}H NMR (500 MHz, $CDCl_3$) δ_H (ppm): 1.10 (d, 3H, $COOCH(CH_3)_2$, J=6.05 Hz), 1.22 (d, 3H,$COOCH(CH_3)_2$, J=6.05 Hz), 2.34 and 2.36 (2s, 6H, C_2–CH_3 and C_6–CH_3), 4.95 (m, 1H, $COOCH(CH_3)_2$), 5.05 and 5.15 (dd, 2H, $COOCH_2$–pyridyl, J=12.65 Hz), 5.08 (s, 1H, DHP–C_4–H), 5.78 (brs, 1H, NH), 7.21–7.24 (m, 1H, pyridyl–H_5), 7.37 (d, 2H, 4-nitro phenyl–$H_{2,6}$, J= 8.3 Hz), 7.49 (d, 1H, pyridyl–H_4, J=7.40 Hz), 8.02 (d, 1H, 4-nitro phenyl–$H_{3,5}$, J= 8.3 Hz), 8.54 (m, 2H, 3-pyridyl–$H_{2,6}$).

MS (EI), *m/z* (%): 451 (M^+, 6), 408 (5), 392 (5), 359 (6), 329 (100), 287 (43), 273 (6), 92 (16.39).

IR (KBr): 3292 (NH), 3081 (CH-aromatic), 2976 (CH-aliphatic), 1679 (C=O), 1516, 1349 (NO_2) cm^{-1}.

2.2.3.4. 3-Pyridin-3-ylmethyl 5-tert-butyl 2,6-dimethyl-4-(4-nitrophenyl)-1,4-dihydropyridine-3,5-dicarboxylate (A4B1). ^{1}H NMR (500 MHz, $CDCl_3$)

δ_H (ppm): 1.40 (s, 9H, $COOC(CH_3)_3$), 2.34 and 2.38 (2s, 6H, C_2–CH_3 and C_6–CH_3), 5.05 (s, 1H, DHP–C_4–H), 5.15 and 5.23 (dd, 2H, $COOCH_2$–pyridyl, J= 13.15 Hz), 6.07 (s, 1H, NH), 7.41 (d, 2H, 4-nitro phenyl–$H_{2,6}$, J= 8.25 Hz), 7.57 (m, 1H, pyridyl–H_5), 7.86 (d, 1H, pyridyl–H_4),8.07 (d, 2H, 4-nitro phenyl–$H_{3,5}$, J= 8.25 Hz), 8.63 (m, 2H, 3-pyridyl–$H_{2,6}$).

MS (EI), m/z (%): 465 (M^+, 5), 408 (20), 392 (5.74), 364 (4.09), 343 (46), 287 (100), 273 (12), 92 (41).

IR (KBr): 3191 (NH), 3075 (CH-aromatic), 2975 (CH-aliphatic), 1704 (C=O), 1512, 1346 (NO_2) cm^{-1}.

2.2.3.5. 3-Pyridin-3-ylmethyl 5-methyl 2,6-dimethyl-4-(3-nitrophenyl)-1,4-dihydropyridine-3,5-dicarboxylate (A1B2). ^{1}H NMR (500 MHz, $CDCl_3$) δ_H (ppm): 2.36 and 2.38 (2s, 6H, C_2–CH_3 and C_6–CH_3), 3.63 (s, 3H, $COOCH_3$), 5.03 and 5.16 (dd, 2H, $COOCH_2$–pyridyl, J=12.55 Hz), 5.08 (s, 1H, DHP–C_4–H), 5.88 (s, 1H, NH), 7.23–7.26 (m, 1H, pyridyl–H_5), 7.32 (t, 1H, 3-nitro phenyl–H_5, J=7.80 Hz), 7.50–7.55 (m, 2H, 3-nitro phenyl–H_6 and pyridyl–H_4), 7.99 (d, 1H, 3-nitro phenyl–H_4, J=7.80 Hz), 8.04 (s, 1H, 3-nitro phenyl–H_2), 8.50 (s, 1H, pyridyl–H_2), 8.55 (d, 1H, pyridyl–H_6).

MS (EI), m/z (%): 423 (M^+, 5), 392 (3), 331 (6), 315 (5), 301 (100), 287 (7), 210 (5), 165 (9.84), 150 (4), 92(20).

IR (KBr): 3298 (NH), 3087 (CH-aromatic), 2958 (CH-aliphatic), 1671 (C=O), 1527, 1346 (NO_2) cm^{-1}.

2.2.3.6. 3-Pyridin-3-ylmethyl 5-ethyl 2,6-dimethyl-4-(3-nitrophenyl)-1,4-dihydropyridine-3,5-dicarboxylate (A2B2). ^{1}H NMR (500 MHz, $CDCl_3$) δ_H (ppm): 1.21 (t, 3H, $COOCH_2CH_3$, J=6.55 Hz), 2.36 and 2.39 (2s, 6H, C_2–CH_3 and C_6–CH_3), 4.08 (q, 2H, $COOCH_2CH_3$, J=6.55 Hz), 5.02 and 5.16 (dd, 2H, $COOCH_2$–pyridyl, J=12.50 Hz), 5.08 (s, 1H, DHP–C_4–H), 5.73 (s, 1H, NH), 7.26 (m, 1H, pyridyl–H_5), 7.32 (t, 1H, 3-nitro phenyl–H_5, J=7.65 Hz), 7.49 (d, 1H, 3-nitro phenyl–H_6, J=7.65 Hz), 7.55 (d, 1H, pyridyl–H_4, J=7.10 Hz), 7.99 (d, 1H, 3-nitro phenyl–H_4, J=7.65 Hz), 8.05 (s, 1H, 3-nitro phenyl–H_2), 8.49 (s, 1H, pyridyl–H_2), 8.54 (brd, 1H, pyridyl–H_6).

MS (EI), m/z (%): 437 (M^+, 5), 392 (4), 364 (4), 345 (6), 315 (100), 301 (5), 287 (6), 269 (4), 151 (6), 92 (21).

IR (KBr): 3292 (NH), 3094 (CH-aromatic), 2982 (CH-aliphatic), 1682 (C=O), 1522, 1343 (NO_2) cm^{-1}.

2.2.3.7. 3-Pyridin-3-ylmethyl 5-isopropyl 2,6-dimethyl-4-(3-nitrophenyl)-1,4-dihydropyridine-3,5-dicarboxylate (A3B2). ^{1}H NMR (500 - MHz, $CDCl_3$) δ_H (ppm): 1.09 (d, 3H, $COOCH(CH_3)_2$, J=6.00 Hz), 1.24 (d, 3H, $COOCH(CH_3)_2$, J=6.00 Hz), 2.35 and 2.38 (2s, 6H, C_2–CH_3 and C_6–CH_3), 4.94 (m, 1H, COOCH(CH3)2), 5.03 and 5.16 (dd, 2H, $COOCH_2$–pyridyl, J=12.60 Hz), 5.07 (s, 1H, DHP–C_4–H), 5.75 (brs, 1H, NH), 7.23–7.26 (m, 1H, pyridyl–H_5), 7.32 (t, 1H, 3-nitrophenyl–H_5, J=7.60 Hz), 7.50 (d, 1H, 3-nitrophenyl–H_6, J=7.25 Hz), 7.55 (d, 1H, pyridyl–H_4, J=7.30 Hz), 7.98 (d, 1H, 3-nitrophenyl–H_4, J=7.60 Hz), 8.05 (s, 1H, 3-nitrophenyl–H_2), 8.49 (s, 1H, pyridyl–H_2), 8.54 (d, 1H, pyridyl–H_6).

MS (EI), m/z (%): 451 (M^+, 5), 408 (3), 392 (5), 364 (6), 329 (100), 287 (50), 273 (8), 243 (5.74), 151 (9), 108 (6), 92 (27).

IR (KBr): 3288 (NH), 3071 (CH-aromatic), 2973 (CH-aliphatic), 1682 (C=O), 1519, 1344 (NO_2) cm^{-1}.

2.2.3.8. 3-Pyridin-3-ylmethyl 5-methyl 2,6-dimethyl-4-(2-nitrophenyl)-1,4-dihydropyridine-3,5-dicarboxylate (A1B3). ^{1}H NMR (500 MHz, $CDCl_3$) δ_H (ppm): 2.31 and 2.34 (2s, 6H, C_2–CH_3 and C_6–CH_3), 3.56 (s, 3H, $COOCH_3$), 5.04 and 5.07 (dd, 2H, $COOCH_2$–pyridyl, J=12.45 Hz), 5.76 (s, 1H, DHP–C_4–H), 5.78 (brs, 1H, NH), 7.18 (m, 1H, 2-nitrophenyl–H_4), 7.26 (m, 1H, pyridyl–H_5), 7.45–7.50 (m, 3H, 2-nitrophenyl–$H_{5,6}$ and pyridyl–H_4), 7.66 (d, 1H, 2-nitrophenyl–H_3, J=7.60 Hz), 8.40 (s, 1H, pyridyl–H_2), 8.48 (d, 1H, pyridyl–H_6).

MS (EI), m/z (%): 423 (M^+ 5), 406 (100), 375 (10), 361 (39), 345 (20), 331 (93), 315 (8), 301 (53), 284 (43), 268 (31), 210 (11), 92 (64).

IR (KBr): 3286 (NH), 3083 (CH-aromatic), 2948 (CH-aliphatic), 1678 (C=O), 1525, 1345 (NO_2) cm^{-1}.

2.2.3.9. 3-Pyridin-3-ylmethyl 5-ethyl 2,6-dimethyl-4-(2-nitrophenyl)-1,4-dihydropyridine-3,5-dicarboxylate (A2B3). ^{1}H NMR (500 MHz, $CDCl_3$) δ_H (ppm): 1.15 (t, 3H, $COOCH_2CH_3$, J=6.90 Hz), 2.32 (s, 6H, C_2–CH_3 and C_6–CH_3), 4.00 (m, 1H, $COOCH_2CH_3$,), 4.12 (m, 1H, $COOCH_2CH_3$,), 5.03 and 5.10 (dd, 2H, $COOCH_2$–pyridyl, J=12.45 Hz), 5.70 (brs, 1H, NH), 5.82 (s, 1H, DHP–C_4–H), 7.19 (m, 1H, 2-nitrophenyl–H_4), 7.26 (m, 1H, pyridyl–H_5), 7.45 (t, 1H, 2-nitrophenyl–H_5, J= 7.25 Hz), 7.50–7.55 (m, 2H, 2-nitrophenyl–H_6 and pyridyl–H_4), 7.69 (d, 1H, 2-nitrophenyl–H_3, J= 7.95 Hz), 8.43 (s, 1H, pyridyl–H_2), 8.49 (rd, 1H, pyridyl–H_6).

MS (EI), m/z (%): 437 (M^+, 6), 420 (100), 361 (33), 345 (100), 331 (7), 315 (52), 298 (26), 284 (22), 270 (28), 254 (17), 226 (18), 92 (84).

IR (KBr): 3286 (NH), 3090 (CH-aromatic), 2969 (CH-aliphatic), 1698, 1678 (C=O), 1528, 1348 (NO_2) cm^{-1}.

2.2.3.10. 3-Pyridin-3-ylmethyl 5-isopropyl 2,6-dimethyl-4-(2-nitrophenyl)-1,4-dihydropyridine-3,5-dicarboxylate (A3B3). ^{1}H NMR (500- MHz, $CDCl_3$) δ_H (ppm): 0.97 (d, 3H, $COOCH(CH_3)_2$, J=6.15 Hz), 1.21 (d, 3H, $COOCH(CH_3)_2$, J=6.15), 2.27 and 2.33 (2s, 6H, C_2–CH_3 and C_6–CH_3), 4.93–4.96 (m, 1H, $COOCH(CH_3)_2$, J=6.15 Hz), 4.99 and 5.12 (dd, 2H, $COOCH_2$–pyridyl, J=12.50 Hz), 5.70 (brs, 1 H, NH), 5.86 (s, 1H, DHP–C_4–H), 7.19–7.22 (m, 1H, 2-nitrophenyl–H_4), 7.23–7.26 (m, 1H, pyridyl–H_5), 7.45 (t, 1H, 2-nitrophenyl–H_5, J=7.65 Hz), 7.51 (d, 1H, 2-nitrophenyl–H_6, J=7.65 Hz), 7.58 (d, 1H, pyridyl–H_4, J=7.55 Hz), 7.72 (d, 1H, 2-nitrophenyl–H_3, J=8.00 Hz), 8.47 (s, 1H, pyridyl–H_2), 8.50 (d, 1H, pyridyl–H_6, J=3.85 Hz).

MS (EI), m/z (%): 451 (M^+ 7), 434 (100), 392 (28), 359 (68), 329 (28), 287 (38), 270 (59), 254 (22), 92 (92), 78 (9).

IR (KBr): 3258(NH), 3064(CH-aromatic), 2982(CH-aliphatic), 1689(C=O), 1530, 1347 (NO_2) cm^{-1}.

2.2.3.11. 3-Pyridin-3-ylmethyl 5-tert-butyl 2,6-dimethyl-4-(2-nitrophenyl)-1,4-dihydropyridine-3,5-dicarboxylate (A4B3). ^{1}H NMR (500- MHz, $CDCl_3$) δ_H (ppm): 1.35 (s, 9H, $COOC(CH_3)_3$), 2.26 and 2.27 (2s, 6H, C_2–CH_3 and C_6–CH_3), 4.98 and 5.14 (dd, 2H, $COOCH_2$–pyridyl, J=12.50 Hz), 5.59 (brs, 1H, NH), 5.79 (s, 1H, DHP–C_4–H), 7.21 (m, 1H, 2-nitrophenyl–H_4), 7.26 (m, 1H, pyridyl–H_5), 7.44 (t, 1H, 2-nitrophenyl–H_5, J=7.60 Hz), 7.50 (d, 1H, 2-nitrophenyl–H_6, J=7.60 Hz), 7.59 (d, 1H, pyridyl–H_4, J=7.50 Hz), 7.68 (d, 1H, 2-nitrophenyl–H_3, J=8.00 Hz), 8.48 (s, 1H, pyridyl–H_2), 8.50 (brd, 1H, pyridyl–H_6, J=3.75 Hz).

MS (EI), m/z (%): 465 (M^+, 0.82), 448 (6), 434 (64), 420 (97), 392(40), 359 (47), 345 (100), 329 (23), 315 (74), 287 (40), 270 (69), 254 (30), 92 (91).

IR (KBr): 3183 (NH), 3067 (CH-aromatic), 2973 (CH-aliphatic), 1692 (C=O), 1529, 1357 (NO_2) cm^{-1}.

2.2.3.12. 3-Pyridin-3-ylmethyl 5-methyl 2,6-dimethyl-4-(1-methyl-5-nitro-1H-imidazol-2-yl)-1,4-dihydropyridine-3,5-dicarboxylate (A1B4). ^{1}H NMR (500 MHz, $CDCl_3$) δ_H (ppm): 2.23 and 2.25 (2s, 6H, C_2–CH_3 and C_6–CH_3), 3.66 (s, 3H, N–CH_3), 3.97 (s, 3H, $COOCH_3$), 5.05 and 5.20 (dd, 2H, $COOCH_2$–pyridyl, J=12.55 Hz), 5.12 (s, 1H, DHP–C_4–H), 7.26 (m, 1H, pyridyl–H_5), 7.53 (d, 1H, pyridyl–H_4, J=7.30 Hz), 7.93 (s, 1 H, imidazole–H), 8.47 (brs, 1H, NH), 8.54 (s, 1H, pyridyl–H_2), 8.58 (d, 1H, pyridyl–H_6, J=3.60 Hz).

MS (EI), m/z (%): 427(M^+, 32), 368(14), 301(41), 291(51), 259 (83), 165(16), 108(41), 92(100).

IR (KBr): 3271 (NH), 3060 (CH-aromatic), 2943 (CH-aliphatic), 1700 (C=O), 1500, 1375 (NO_2) cm^{-1}.

2.2.3.13. 3-Pyridin-3-ylmethyl 5-ethyl 2,6-dimethyl-4-(1-methyl-5-nitro-1H-imidazol-2-yl)-1,4-dihydropyridine-3,5-dicarboxylate (A2B4). ^1H NMR (500 MHz, $CDCl_3$) δ_H (ppm): 1.23 (t, 3H, $COOCH_2CH_3$, J=7.00 Hz), 2.23 and 2.24 (2s, 6H, C_2–CH_3 and C_6–CH_3), 3.99 (s, 3H, N–CH_3), 4.12 (q, 2H, $COOCH_2CH_3$, J=7.00 Hz), 5.06 and 5.21 (dd, 2H, $COOCH_2$–pyridyl, J=12.55 Hz), 5.13 (s, 1H, DHP–C_4–H), 7.26 (m, 1H, pyridyl–H_5), 7.53 (d, 1H, 1H, pyridyl–H_4, J=7.50 Hz), 7.92 (s, 1 H, imidazole–H), 8.54 (brs, 2H, NH and pyridyl–H_2), 8.58 (d, 1H, pyridyl–H_6, J=3.80 Hz).

MS (EI), m/z (%): 441 (M^+, 37), 424 (4.46), 396 (4), 368 (23), 305 (39), 287 (11), 259 (100), 92 (63).

IR (KBr): 3270 (NH), 3058 (CH-aromatic), 2973 (CH-aliphatic), 1697 (C=O), 1500, 1375 (NO_2) cm^{-1}.

2.2.3.14. 3-Pyridin-3-ylmethyl 5-isopropyl 2,6-dimethyl-4-(1-methyl-5-nitro-1H-imidazol-2-yl)-1,4-dihydropyridine-3,5-dicarboxylate (A3B4). ^1H NMR (500 MHz, $CDCl_3$) δ_H (ppm): 1.18 (d, 3H, $COOCH(CH_3)_2$, J=6.10 Hz), 1.21 (d, 3H, $COOCH(CH_3)_2$, J=6.10 Hz), 2.24 and 2.25 (2s, 6H, C_2–CH_3 and C_6–CH_3), 4.02 (s, 3H, N–CH_3), 5.00 (m, 1H, $COOCH(CH_3)_2$, J=6.10 Hz), 5.06 and 5.21 (dd, 1H, $COOCH_2$–pyridyl, J=12.55 Hz), 5.11 (s, 1H, DHP–C_4–H), 7.26 (m, 1H, pyridyl–H_5), 7.53 (d, 1H, pyridyl–H_4, J=7.45 Hz), 7.92 (s, 1H, imidazole–H), 8.18 (brs, 1H, NH), 8.54 (s, 1H, pyridyl–H_2), 8.58 (d, 1H, pyridyl–H_6, J=3.80 Hz).

MS (EI), m/z (%): 455 (M^+ 33), 396 (6), 368 (51), 319 (24), 287 (27), 259 (100), 233 (20), 92 (62).

IR (KBr): 3268 (NH), 3051 (CH-aromatic), 2977 (CH-aliphatic), 1700 (C=O), 1503, 1373 (NO_2) cm^{-1}.

2.2.3.15. 3-Pyridin-3-ylmethyl 5-tert-butyl 2,6-dimethyl-4-(1-methyl-5-nitro-1H-imidazol-2-yl)-1,4-dihydropyridine-3,5-dicarboxylate (A4B4). ^1H NMR (500 MHz, $CDCl_3$) δ_H (ppm): 1.41 (s, 9H, $COOC(CH_3)_3$), 2.17 and 2.25 (2s, 6H, C_2–CH_3 and C_6–CH_3), 3.99 (s, 3H, N–CH_3), 5.05 and 5.19 (dd, 2H, $COOCH_2$–pyridyl, J=12.55 Hz), 5.09 (s, 1H, DHP–C_4–H), 7.26 (m, 1H, pyridyl–H_5), 7.52 (d, 1H, pyridyl–H_4, J= 7.40 Hz), 7.92 (s, 1H, imidazole–H (, 8.33 (brs, 1H, NH), 8.57 (s, 1H, pyridyl–H_2), 8.57 (d, 1H, pyridyl–H_6, J=3.80 Hz).

MS (EI), m/z (%): 469 (M^+, 16), 396 (8), 368 (69), 352 (24), 287 (42), 260 (78), 233 (63), 92 (76.23), 57 (100).

IR (KBr): 3278 (NH), 3056 (CH-aromatic), 2972 (CH-aliphatic), 1705, 1671 (C=O), 1517, 1373 (NO_2) cm^{-1}.

2.2.3.16. 3-Pyridin-3-ylmethyl 5-methyl 2,6-dimethyl-4-(thiophen-2-yl)-1,4-dihydropyridine-3,5-dicarboxylate (A1B5). ^1H NMR (500 MHz, $CDCl_3$) δ_H (ppm): 2.33 and 2.36 (2s, 6H, C_2–CH_3 and C_6–CH_3), 3.71 (s, 3H, $COOCH_3$), 5.10 and.25(dd, 2H, $COOCH_2$–pyridyl, J=13.00 Hz), 5.35 (s, 1H, DHP–C_4–H), 6.02 (brs, 1H, NH), 6.75 (d, 1H, thiophenyl–H_3), 6.84 (t, 1H, thiophenyl–H_4), 7.06 (d, 1H, thiophenyl–H_5, J= 4.60 Hz), 7.23 (m, 1H, pyridyl–H_5), 7.52 (d, 1H, pyridyl–H_4, J= 7.45 Hz), 8.26 (s, 2H, pyridyl–$H_{2,6}$).

MS (EI), m/z (%): 384 (M^+, 40), 353 (7), 325 (45), 292 (87), 248 (100), 218 (13), 165 (16), 150 (15), 108 (15), 92 (74).

IR (KBr): 3332 (NH), 3070 (CH-aromatic), 2947 (CH-aliphatic), 1698 (C=O) cm^{-1}.

2.2.3.17. 3-Pyridin-3-ylmethyl 5-ethyl 2,6-dimethyl-4-(thiophen-2-yl)-1,4-dihydropyridine-3,5-dicarboxylate (A2B5). ^1H NMR (500 MHz, $CDCl_3$) δ_H (ppm): 1.28 (t, 3H, $COOCH_2CH_3$, J=7.15 Hz), 2.33 and 2.37 (2s, 6H, C_2–CH_3 and C_6–CH_3), 4.18 (q, 2H, $COOCH_2CH_3$, J=7.15 Hz), 5.12 and 5.24 (dd, 2H, $COOCH_2$–pyridyl, J=12.90 Hz), 5.38 (s, 1H, DHP–C_4–H), 5.83 (brs, 1H, NH), 6.76 (brd, 1H, thiophenyl–H_3), 6.84 (t, 1H, thiophenyl–H_4), 7.06 (d, 1H, thiophenyl–H_5, J= 4.6 Hz), 7.23 (m, 1H, pyridyl–H_5), 7.53 (d, 1H, pyridyl–H_4, J=7.45 Hz), 8.53 (s, 2H, pyridyl–$H_{2,6}$).

MS (EI), m/z (%): 398 (M^+, 45), 353 (11), 325 (86), 306 (100), 278 (18), 262 (85), 234 (16), 218 (27), 150 (26), 92 (58).

IR (KBr): 3298 (NH), 3095 (CH-aromatic), 2979 (CH-aliphatic), 1676 (C=O) cm^{-1}.

2.2.3.18. 3-Pyridin-3-ylmethyl 5-isopropyl 2,6-dimethyl-4-(thiophen-2-yl)-1,4-dihydropyridine-3,5-dicarboxylate (A3B5). ^1H NMR (500 MHz, $CDCl_3$) δ_H (ppm): 1.22 (d, 3H, $COOCH(CH_3)_2$, J=6.10 Hz), 1.26 (d, 3H, $COOCH(CH_3)_2$), J=6.10 Hz), 2.32 and 2.36 (2s, 6H, C_2–CH_3 and C_6–CH_3), 5.04 (m, 1H, $COOCH(CH_3)_2$), 5.13 and 5.23 (dd, 2H, $COOCH_2$–pyridyl, J=12.95 Hz), 5.37 (s, 1H, DHP–C_4–H), 5.87 (brs, 1H, NH), 6.76 (brd, 1H, thiophenyl–H_3), 6.83 (t, 1H, thiophenyl–H_4), 7.05 (d, 1H, thiophenyl–H_5, J=4.60 Hz), 7.23 (m, 1H, pyridyl–H_5),7.54 (d, 1H, pyridyl–H_4, J=7.45 Hz), 8.53 (s, 2H, pyridyl–$H_{2,6}$).

MS (EI), m/z (%): 412 (M^+, 41), 369 (14), 325 (100), 287 (38), 234 (46), 188 (12.29), 150 (19.67), 92 (32).

IR (KBr): 3293 (NH), 3090 (CH-aromatic), 2981 (CH-aliphatic), 1688 (C=O) cm^{-1}.

2.3. Calcium channel blocking activity

In vitro CCB activity of synthesized compounds was evaluated on guinea pig ileal longitudinal smooth muscle (GPILSM) as previously described with some modifications (Mehdipour et al., 2007; Miri et al., 2007). Male albino guinea pigs were obtained from Animal House Department of Shiraz University of Medical Sciences. The animals were fasted overnight before the test. They were sacrificed and their intestines were removed above the ileocecal junction. Ileum was cut into about 1 cm segments and segments were kept at 4 °C for 6–16 h in oxygenated physiological saline solution of the following compositions: NaCl 119 mM, KCl 2.70 mM, $CaCl_2 \cdot 02H_2O$ 2.00 mM, $MgCl_2 \cdot 06H_2o$ 0.88 mM, NaH_2PO_4 0.36 mM, $NaHCO_3$ 12.00 mM and glucose 5.50 mM. Afterwards, muscle segments were mounted in 5 ml Jacketed organ bath (Letica, Spain) containing oxygenated physiological saline solution at 37 °C, under a resting tension of 0.5 g. The ileal muscle contractions were recorded with a forced displacement transducer (Hugo Sachs, March-Hugstetten and Germany) on a physiograph (Hugo Sachs). The contraction was induced with 40 mM KCl and the KCl-induced contraction was considered as 100% value. Synthesized compounds and nifedipine (the positive control) were added at the final concentrations of 10^{-10}, 10^{-9}, 10^{-8}, 10^{-7}, 10^{-6} and 10^{-5} M for evaluation of their inhibitory effect on muscle contraction and after 10 min KCl was added to induce contraction. The IC_{50} value of each compound was calculated from concentration–response curve.

2.4. Cell lines

Six cell lines were used in this study including HL-60 (acute promyelocytic leukemia), K562 (chronic myelogenous leukemia), MCF-7 (human breast adenocarcinoma), LS180 (human colon adenocarcinoma), MES-SA/DX-5 (human uterine sarcoma with P-gp over-expression) and its parental cell line MES-SA. All cell lines were obtained from the National Cell Bank of Iran, Pasteur Institute, Tehran, Iran. Cells were cultured in RPMI 1640 supplemented with 10% FBS (20% FBS for HL-60 cell line) and 100 units/ml penicillin-G and 100 ug/ml streptomycin at 37 °C in humidified air containing 5% CO_2. K562 and HL-60 cell lines were grown in suspension, while MCF-7, LS180, MES-SA and MES-SA/DX5 cells were grown in monolayer culture.

2.5. Cytotoxicity assay

In vitro cytotoxic activity of synthesized compounds was evaluated by MTT reduction assay (Jassbi et al., 2014; Mosmann, 1983). Cells at the logarithmic phase were seeded into 96-well plates with 3–5 × 10^3 cells/well (depending on the cell line) and incubated for 24 h at 37 °C. Then, four different concentrations of synthesized compounds, cisplatin and doxorubicin (as positive controls) were added in triplicate and plates were incubated at 37 °C for another 72 h. After the incubation period, 80 µl of media was removed from each well and 80 µl of MTT solution in phosphate-buffered saline at a concentration of 5 mg/ml was added for MTT assay (Plates with suspension cells were centrifuged before the procedure). After 4 h incubation and formation of formazan crystals, 200 µl DMSO was added to dissolve crystals. Finally absorbance was measured at a wavelength of 570 nm with background correction at 650 nm using a microplate reader (model 680, Bio-Rad, Japan) and IC_{50} (concentration that results in 50% inhibition of cell viability) for each compound was calculated with Curve Expert version 1.34 for windows.

2.6. Measurement of rhodamine 123 efflux by flow cytometry

To measure the inhibition of rhodamine 123 (Rh123) efflux from MES-SA/DX5 cells by synthesized compounds, as an index of P-gp function modulation, a previously described method was used with some modifications (Munić et al., 2010; Wesolowska et al., 2005; Xi et al., 2010). Tubes containing MES-SA/DX5 cells (5 × 10^5 cells/ml) in RPMI 1640 medium without phenol-red were treated with 5 µM Rh123 for 30 min at 37 °C. Afterwards cells were centrifuged and washed twice with ice-cold PBS and resuspended in RPMI 1640 medium containing verapamil (positive control) or synthesized compounds as P-gp inhibitors. Tubes were incubated for 30 min at 37 °C.

The fluorescence emission caused by the presence of Rh123 in cells was measured by a FACSCalibur flow cytometer (Becton Dickenson, USA) with an excitation and emission wavelengths of 488 and 530 nm, respectively. Geometric mean (Gmean) of fluorescence intensity values was determined using WINMDI 2.9 (TSRI, USA).

2.7. MDR reversal assay

MDR reversal activity of synthesized compound was evaluated on MES-SA/DX5 cell line (MDR subline of MES-SA cell line) by MTT assay. At first, 4 × 10^3 cells/well were seeded into 96-well plates and incubated for 24 h at 37 °C. Afterwards, two different concentrations of synthesized compounds, which had no cytotoxic activity (cells viability > 90%), were added in triplicate followed by the addition of 3 different concentration of doxorubicin after 1 h. After 72 h of incubation, MTT assay was performed as described in Section 2.5.

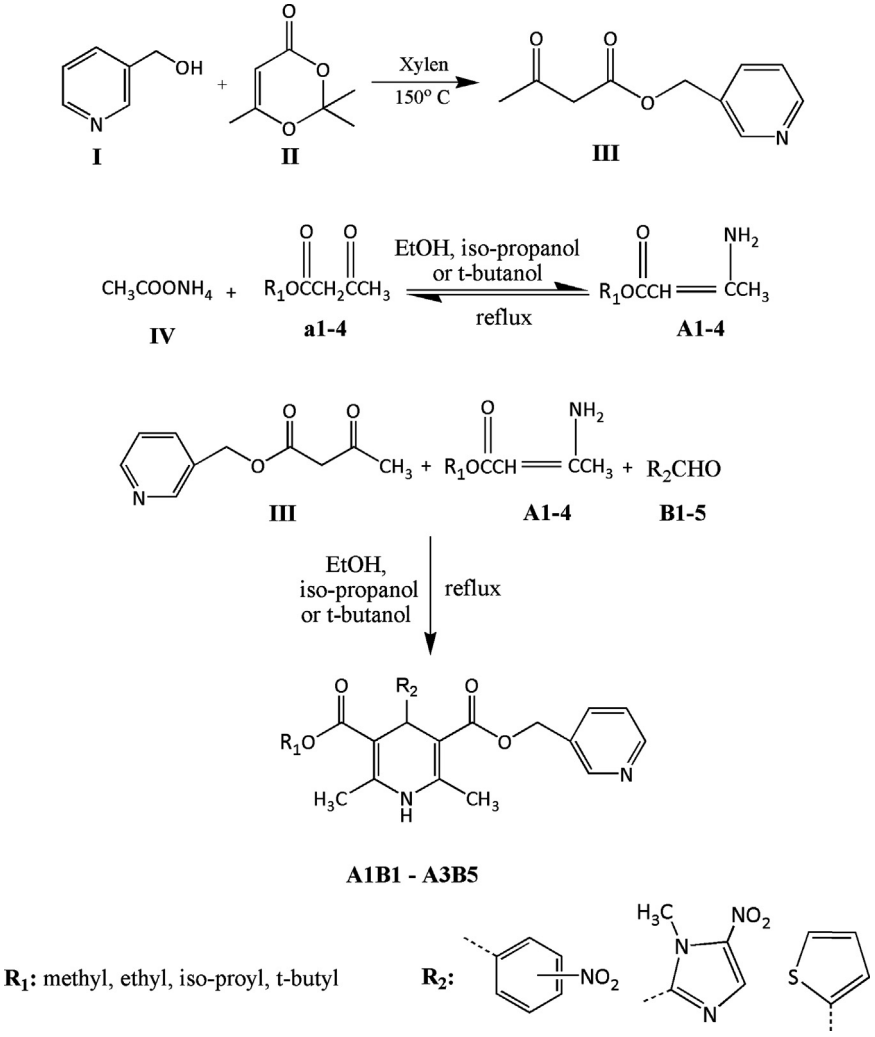

Scheme 1. Synthetic pathway of 1,4-DHP derivatives (A1B1-A3B5).

Finally, percentage of IC_{50} reduction of doxorubicin was calculated as $100 \times (IC_{50\ doxorubicin} - IC_{50doxorubicin+DHP})/IC_{50doxorubicin}$.

2.8. Western blot analysis of P-gp expression

Protein extraction from MES-SA/DX5 and MES-SA cells was carried out by RIPA buffer containing protease inhibitor cocktail and PMSF (phenylmethylsulfonyl fluoride) 10 μM. Cell lysates were centrifuged at 16,000*g* for 30 min and the supernatants were collected and kept at −20 °C before analysis. Bradford assay was used for the determination of protein concentrations in the protein extracts. Samples were loaded onto SDS polyacrylamide gel (7.5%) and separated by the electrophoresis process. Then the proteins were transferred to polyvinylidene difluoride (PVDF) membranes in a Mini-Protean III transfer system (Bio-Rad, CA, USA) and immunoblotted with a mouse monoclonal anti P-gp antibody (C219, Calbiochem, Germany). Afterwards, the membrane was incubated with goat anti-mouse secondary antibody conjugated to horseradish peroxidase (Santa Cruz Biotechnologies, USA). Finally immunoreactions were detected by ECL (Pierce, Rockford, USA) and the images were taken by a Syngene G: box gel doc.

3. Results

3.1. Chemistry

Asymmetrical 1,4-dihydropyridine (1,4-DHP) derivatives A1B1-A3B5 were synthesized as described in Section 2.2. (Scheme 1). Pyridin-3-yl-methyl-3-oxobutanoate III was prepared through the reaction of corresponding alcohol I with 2,2,6-trimethyl-4-H-1,3-dioxin-4-one II. A mixture of ammonium acetate IV and alkylacetoacetate a1–4 were refluxed in suitable solvent to produce alkyl 3-aminocrotonate A1–4. Final DHP derivatives were synthesized *via* the reaction of pyridin-3-yl-methyl-3-oxobutanoate III, alkyl 3-aminocrotonate A1–4 and aryl or heteroaryl aldehydes B1–5. Chemical structures of synthesized compounds along with their physical data are listed in Table 1.

3.2. Calcium channel blocking activity

1,4-DHP derivatives are a known class of CCB agents and are among the most commonly used cardiovascular drugs. In this study, the IC_{50} value of each synthesized DHP compound (concentration that results in 50% inhibition of smooth muscle contractility) was determined in guinea pig ileal longitudinal smooth muscle (GPLISM) as a potential side effect when these agents are applied as MDR reversal and cytotoxic drugs (Table 2).

Based on our findings, compounds A1B4–A4B4 (bearing 1-methyl-5-nitro-imidazole-2-yl moiety at C_4 position) exhibited the weakest activities ($IC_{50} = 10^{-5} - 10^{-6}$ M), while the highest CCB activity belonged to A1B2, A3B2 and A3B3, which were comparable with nifedipine as a reference drug ($IC_{50} = 6.89 \times 10^{-8}$ M).

3.3. Cytotoxicity assay

The intrinsic cytotoxic activities of compounds were evaluated on HL-60, K562, MCF-7 and LS180 cell lines. Doxorubicin and cisplatin were also tested as positive controls. IC_{50} values are shown in Table 3.

Tested compounds seemed in general to have stronger cytotoxic effects on HL-60 and K562 cell lines, while their effects on LS180 cell line appeared to be weaker. The lowest IC_{50} belonged to A2B5 (IC_{50} range: 1.06–4.12 μM) and A2B2 (IC_{50} range: 3.77–15.60 μM), which had 2-thienyl and 3-nitrophenyl at C_4 position, respectively. A2B5 was stronger than cisplatin, which was tested as a positive control in all cell lines (IC_{50} range: 2.93–14.67 μM). In all tested compounds, except for A3B2 and A3B5, the increase in the size of alkyl chain at C_5 position potentiated the cytotoxic activity. A3B2 and compounds with 1-methyl-5-nitro-imidazole-2-yl moiety at C_4 position (A1B4 to A4B4) had mostly IC_{50} values of

Table 1
Chemical structures and physical properties of synthesized 1,4-dihydropyridine compounds.

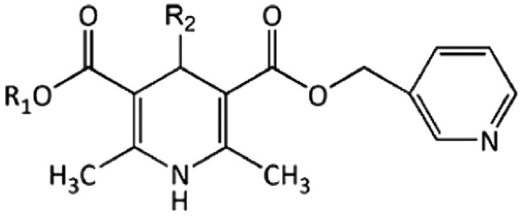

Compound	R_1	R_2	Melting point (°C)	Yield (%)	R_f
A1B1	Methyl	4-nitrophenyl	193–194	21.2	0.32
A2B1	Ethyl	4-nitrophenyl	118–120	13.1	0.32
A3B1	Isopropyl	4-nitrophenyl	137–138	10.1	0.36
A4B1	t-Butyl	4-nitrophenyl	147–150	7.0	0.34
A1B2	Methyl	3-nitrophenyl	171–172	12.2	0.36
A2B2	Ethyl	3-nitrophenyl	153–155	17.5	0.40
A3B2	Isopropyl	3-nitrophenyl	185–189	14.1	0.38
A1B3	Methyl	2-nitrophenyl	166–170	9.7	0.30
A2B3	Ethyl	2-nitrophenyl	136–137	7.1	0.28
A3B3	Isopropyl	2-nitrophenyl	136–138	19.5	0.30
A4B3	t-butyl	2-nitrophenyl	131–133	3.8	0.28
A1B4	Methyl	1-methyl-5-nitro-imidazole-2-yl	Decomposed at 208	6.2	0.28
A2B4	Ethyl	1-methyl-5-nitro-imidazole-2-yl	Decomposed at 211	7.1	0.26
A3B4	Isopropyl	1-methyl-5-nitro-imidazole-2-yl	201–204	16.7	0.28
A4B4	t-Butyl	1-methyl-5-nitro-imidazole-2-yl	Decomposed at 208	11.2	0.26
A1B5	Methyl	2- thienyl	86–89	5.5	0.24
A2B5	Ethyl	2- thienyl	95–96	4.8	0.28
A3B5	Isopropyl	2- thienyl	102–104	5.7	0.28

higher than 100 μM and were the weakest agents against all cancer cell lines.

3.4. Flow cytometric measurement of rhodamine 123 efflux

Rh123 is a known fluorescent substrate for P-gp and is pumped out of the cell by this transporter (Twentyman et al., 1994). The capacity of synthesized compounds to inhibit P-gp pump was evaluated by Rh123 efflux in MES-SA/DX5 cells and results are shown in Figs. 1 and 2.

According to the obtained data, most of the DHP compounds, especially those possessing nitrophenyl at C_4 position (A1B1 to A4B3), induced a significant increase in Geometric mean (Gmean) of fluorescence intensity compared to control at 5–25 μM (Fig. 2 A–C, P value < 0.05). Gmean of fluorescence intensity corresponds to the amount of Rh123 retained inside the cells and is directly correlated with P-gp inhibition. The highest Gmean values belonged to A2B2, A3B2, A3B1 and A4B1 were the most effective compounds. Compound A2B2 (with Gmeans of 56.97 ± 5.9 and 62.90 ± 11.42 at 10 and 25 μM, respectively), was more active than verapamil (with Gmeans of 43.50 ± 4.71 and 48.54 ± 0.89 at 10 and 25 μM, respectively) as a reference P-gp inhibitor compound. Similarly, A3B2 and A3B1, at the concentration of 10 and 25 μM, were more effective than verapamil at the same concentrations. Generally, the compounds with 3-nitrophenyl (A1B2 to A3B2) or 4-nitrophenyl (A1B1 to A4B1) at C_4 position showed greater P-gp inhibitory activities, while derivatives with 1-methyl-5-nitro-imidazole-2-yl moiety at C_4 position (A1B4 to A4B4) showed the lowest activities.

Table 2
Calcium channel blocking activity of synthesized 1,4-DHP derivatives.

Compound	$IC_{50} \pm$ S.E.M. (M)	P value
A1B1	$(3.5 \pm 2.8) \times 10^{-7}$	0.99
A2B1	$(5.1 \pm 3.4) \times 10^{-7}$	0.87
A3B1	$(8.2 \pm 2.9) \times 10^{-7}$	0.04[a]
A4B1	$(3.0 \pm 1.4) \times 10^{-6}$	0.00[a]
A1B2	$(4.9 \pm 2.0) \times 10^{-8}$	1.00
A2B2	$(5.5 \pm 4.7) \times 10^{-7}$	0.78
A3B2	$(2.9 \pm 1.1) \times 10^{-8}$	0.97
A1B3	$(1.5 \pm 0.6) \times 10^{-7}$	0.99
A2B3	$(1.6 \pm 0.8) \times 10^{-7}$	0.98
A3B3	$(6.0 \pm 2.2) \times 10^{-8}$	1.00
A4B3	$(8.0 \pm 3.8) \times 10^{-7}$	0.10
A1B4	$(1.2 \pm 0.9) \times 10^{-5}$	0.00[a]
A2B4	$(1.6 \pm 0.9) \times 10^{-6}$	0.01[a]
A3B4	$(9.6 \pm 4.0) \times 10^{-6}$	0.00[a]
A4B4	$(4.7 \pm 1.9) \times 10^{-6}$	0.00[a]
A1B5	$(2.8 \pm 1.8) \times 10^{-6}$	0.01[a]
A2B5	$(9.6 \pm 3.4) \times 10^{-7}$	0.05[a]
A3B5	$(2.9 \pm 1.5) \times 10^{-7}$	0.57
Nifedipine	$(6.9 \pm 2.8) \times 10^{-8}$	

[a] Difference between the IC50 value of the compound and nifedipine (as positive control) was significant ($P < 0.05$). $n=4$.

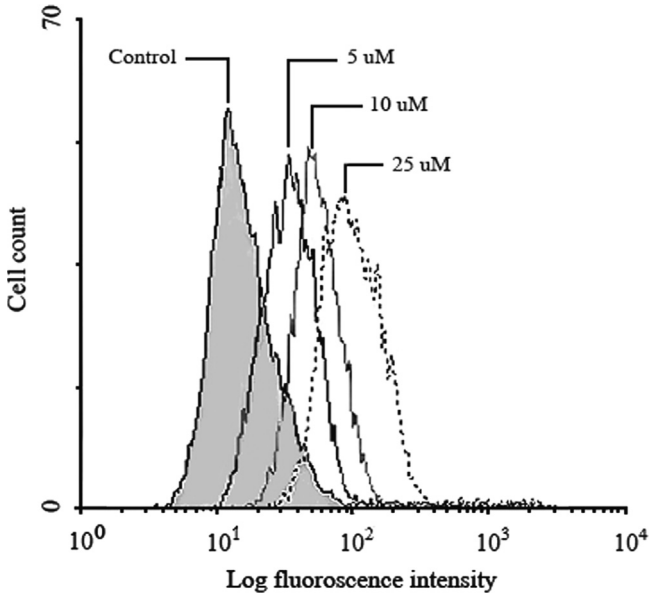

Fig. 1. Effect of compound A2B2 on the retention of rhodamine 123 in MES-SA/DX5 cells. Rh123 5 μM was added to tubes containing 5×10^5 MES-SA/DX5 cells and incubated for 30 min at 37 °C. Afterwards cells were centrifuged and washed twice with ice-cold PBS and resuspended in RPMI 1640 medium containing A2B2 as P-gp inhibitor. After 30 min of incubation at 37 °C, 10,000 cells were counted by a flow cytometer with excitation and emission wavelengths of 488 nm and 530 nm, respectively. Finally histograms were drawn by WINMDI version 2.9.

Table 3
Cytotoxic activities of synthesized 1,4-DHP derivatives against human cancer cell lines.

Compound	IC_{50} (μM) $\pm$ S.E.M. ($n=4$)			
	HL-60	K562	MCF-7	LS180
A1B1	45.08 ± 3.0	40.34 ± 4.5	51.80 ± 3.2	71.28 ± 1.4
A2B1	30.06 ± 0.6	21.15 ± 2.4	34.30 ± 2.5	37.01 ± 3.1
A3B1	26.51 ± 2.0	17.40 ± 1.8	26.45 ± 2.4	34.71 ± 2.7
A4B1	23.75 ± 1.8	15.49 ± 1.2	21.47 ± 0.7	27.65 ± 2.6
A1B2	8.34 ± 0.5	9.11 ± 2.2	16.42 ± 1.3	18.67 ± 2.6
A2B2	3.77 ± 0.4	8.29 ± 1.9	15.60 ± 2.1	11.39 ± 1.5
A3B2	> 100	> 100	> 100	> 100
A1B3	64.44 ± 2.7	70.64 ± 7.5	71.61 ± 8.1	61.22 ± 10.8
A2B3	55.92 ± 4.74	47.90 ± 4.6	54.29 ± 6.4	57.93 ± 10.3
A3B3	33.65 ± 0.4	38.26 ± 6.2	27.86 ± 1.3	49.22 ± 2.6
A4B3	27.47 ± 0.8	26.25 ± 3.1	26.13 ± 2.4	41.86 ± 0.1
A1B4	> 100	> 100	> 100	> 100
A2B4	> 100	> 100	> 100	> 100
A3B4	> 100	> 100	> 100	> 100
A4B4	59.30 ± 7.07	68.87 ± 7.7	62.85 ± 3.4	> 100
A1B5	16.20 ± 0.3	15.38 ± 1.9	23.62 ± 4.4	50.39 ± 4.5
A2B5	1.06 ± 0.0	2.61 ± 0.8	4.12 ± 0.7	3.37 ± 0.1
A3B5	13.65 ± 0.4	7.89 ± 0.4	18.81 ± 2.4	26.22 ± 0.6
Cisplatin	2.93 ± 0.2	11.84 ± 1.3	11.94 ± 2.2	14.67 ± 2.7
Doxorubicin	$(5.8 \pm 0.3) \times 10^{-3}$	$(63.0 \pm 3.5) \times 10^{-3}$	$(45.7 \pm 5.1) \times 10^{-3}$	$(85.1 \pm 22.1) \times 10^{-3}$

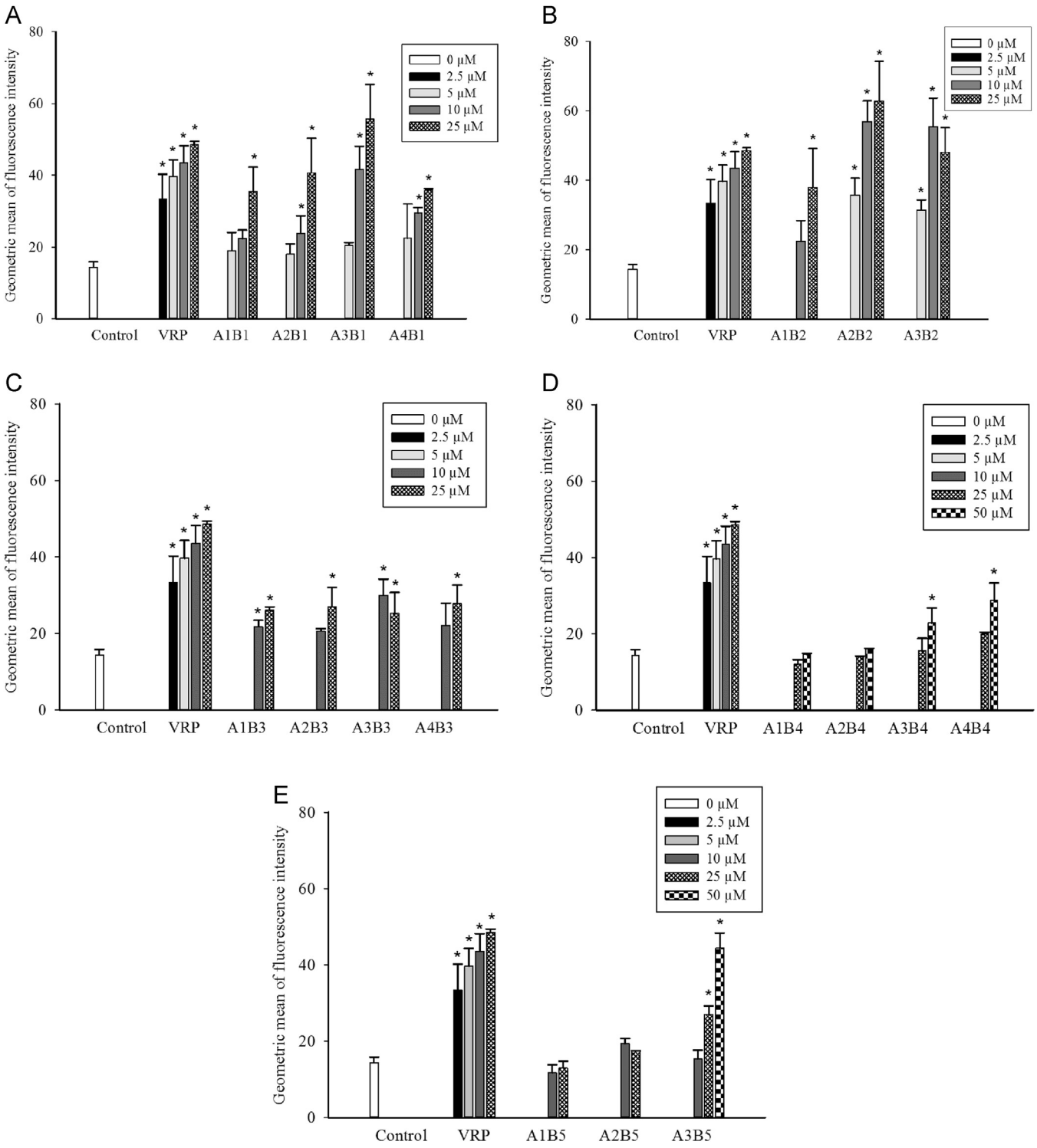

Fig. 2. Flow cytometric detection of rhodamine 123 efflux from MES-SA/DX5 cells. Retention of Rh123 in MES-SA/DX5 cells was measured by flow cytometry. Cells were exposed to 5 μM Rh123 for 30 min at 37 °C and then centrifuged and washed twice with ice-cold PBS and resuspended in RPMI 1640 containing verapamil (positive control) or synthesized compounds as P-gp inhibitors. After 30 min of incubation at 37 °C, the fluorescence caused by the presence of Rh123 in cells was measured by a flow cytometer with excitation and emission wavelengths of 488 nm and 530 nm, respectively. Effects of synthesized compounds with 4-nitrophenyl (A), 3-nitrophenyl (B), 2-nitrophenyl (C), 1-methyl-5-nitro-imidazole-2-yl (D) and 2-thienyl (E) at C_4 position and verapamil as a positive control are shown. VRP: verapamil, * shows that the difference between Gmean of fluoroscence intensities in the absence and presence of the test compound is significant ($P < 0.05$).

3.5. MDR reversal assay

MDR reversal activity of synthesized compounds was evaluated in MES-SA/DX5 cells. The compounds were also tested in MES-SA parental non-resistant cell line for comparison. DHPs under study had no inherent cytotoxicity at the tested concentrations (cell viability > 90%, data not shown). Results are presented in Figs. 3–5.

A3B2 which has 3-nitrophenyl at C_4 was the most effective compound, significantly lowering the IC_{50} of doxorubicin in MES-

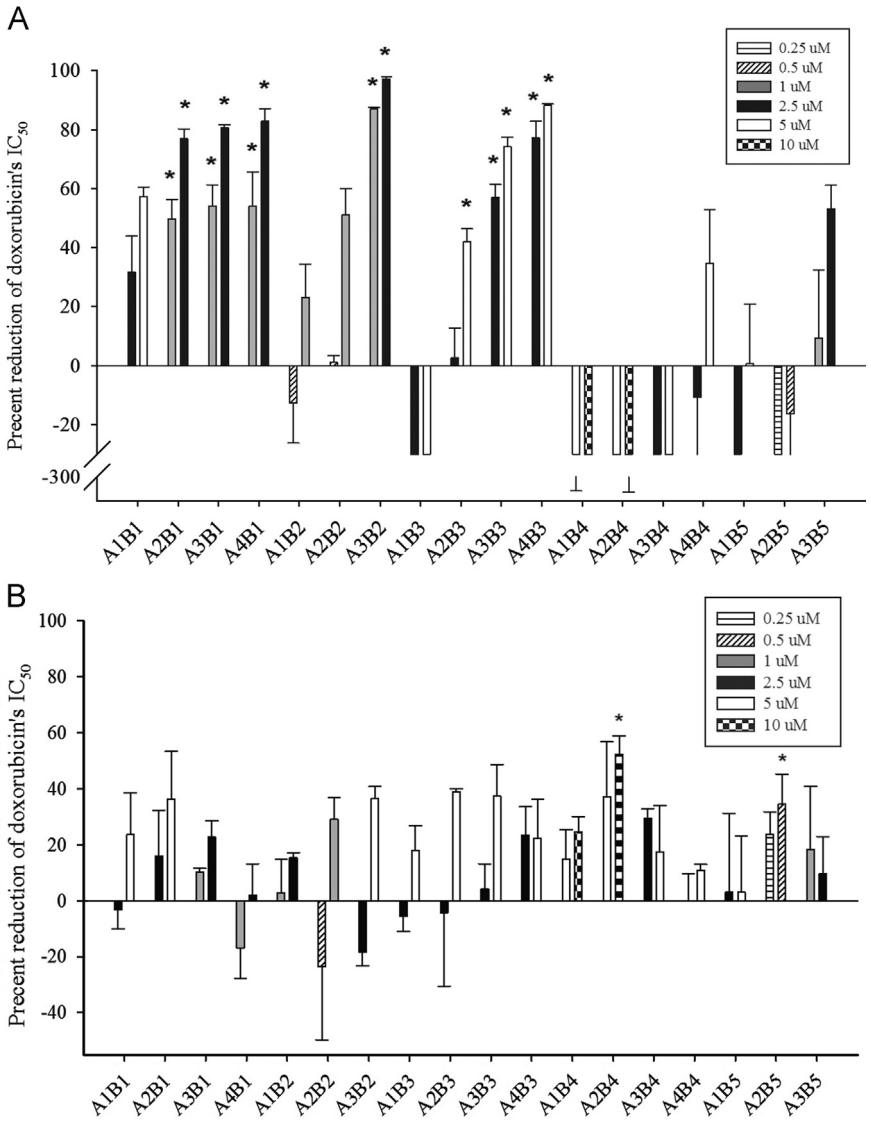

Fig. 3. Measurement of doxorubicin resistance reversal in MES-SA/DX5 and MES-SA cells. Reduction of doxorubicin's IC_{50} by synthesized compounds was evaluated in MES-SA/DX5 (A) and MES-SA cell lines (B). Cells were seeded in 96-well microplates and after overnight incubation; they were consecutively treated with two different concentrations of DHPs followed by doxorubicin. Plates were further incubated for 72 h, MTT assay was carried out and IC_{50} of doxorubicin was calculated in the absence or presence of synthesized compounds and percent reduction of IC_{50} values were calculated. * shows that the difference between the IC_{50} values of doxorubicin in the absence and presence of the test compounds is significant ($P < 0.05$).

SA/DX5 cells at 1 μM (Fig. 3A and Fig. 4D). This compound reduced the IC_{50} of doxorubicin to 21.8 μM (data not shown), a similar value to MES-SA cells, which could be interpreted as complete reversal of MDR in resistant cells. Most of the synthesized compounds possessing nitrophenyl at C_4 position (A1B1 to A4B3) significantly increased the cytotoxicity of doxorubicin on MES-SA/DX5 cells at 1–5 μM, while they had no significant effect on MES-SA cells at similar concentrations. Among the nitrophenyl bearing compounds at C_4, the presence of 4-nitrophenyl seemed to confer a higher activity as seen in A2B1, A3B1 and A4B1 (Fig. 3A and Fig. 4). On the other hand, replacement of nitrophenyl with hetero aromatic moieties at C_4 (in A1B4 to A3B5) caused a reduction of MDR reversal activity.

3.6. Western blot analysis of P-gp expression

P-gp expression in MES-SA/DX5 and its parental cell line MES-SA was examined by immunoblottiong. The results showed that MES-SA/DX5 cells over-express P-gp, while the level of P-gp in MES-SA was not detectable (Fig. 6).

4. Discussion

In this study, 18 novel asymmetrical 1,4-DHP derivatives were synthesized and assessed for cytotoxicity in 4 human cancer cell lines and MDR reversal activity through P-gp modulation in doxorubicin resistant cells and their SAR was examined. SAR studies are of utmost importance for drug discovery in order to determine the important structural features required for higher pharmacological activities (Kumar et al., 2014; Singhuber et al., 2011).

CCB activity of synthesized DHPs was determined as a potential cardiovascular side effect of these compounds. Among compounds bearing nitrophenyl moiety at C_4 position, compounds with 4-nitrophenyl were weaker CCB agents compared to those having 2-nitrophenyl or 3-nitrophenyl. These findings are in accordance

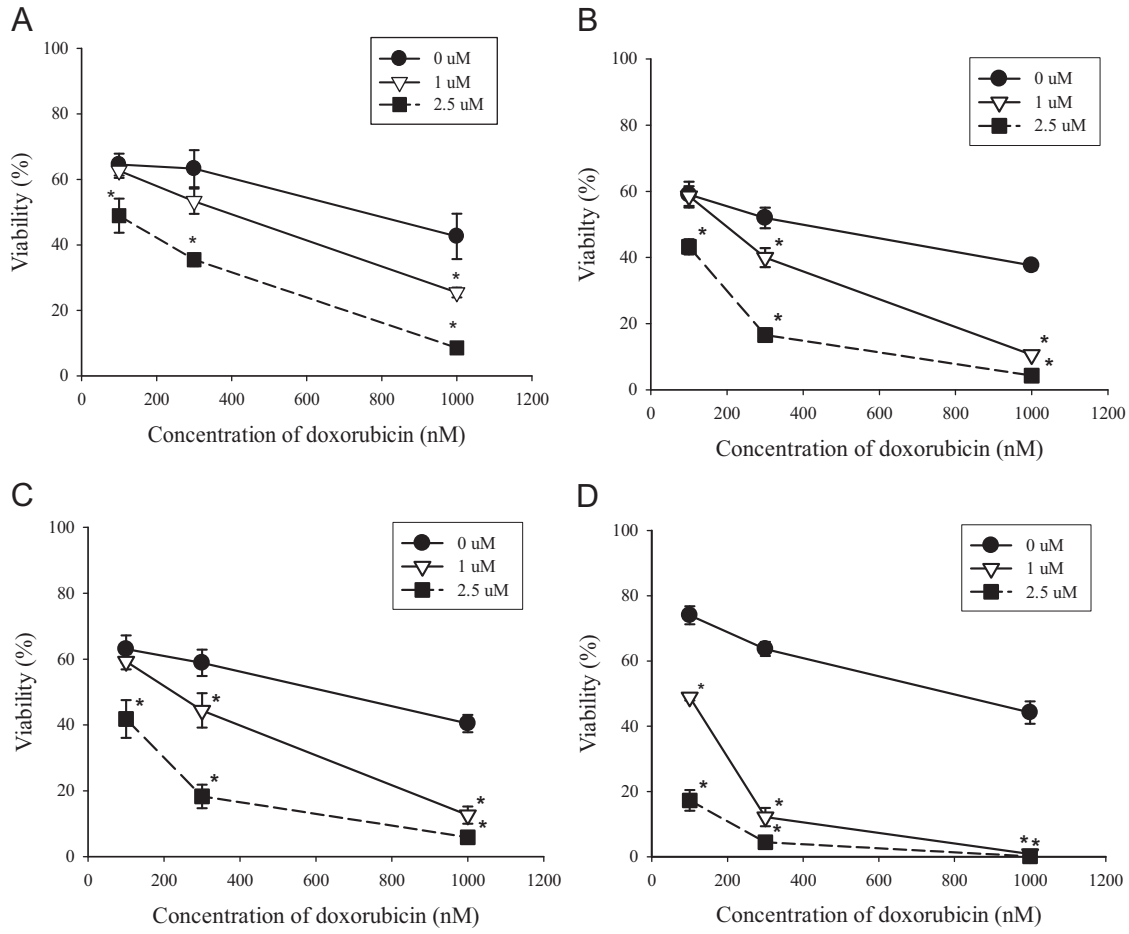

Fig. 4. Multidrug resistance reversal in MES-SA/DX5 cells. Effect of doxorubicin on the viability of MES-SA/DX5 cells (doxorubicin-resistant) in the absence or presence of the most potent MDR reversal compounds A2B1 (A), A3B1 (B), A4B1 (C) and A3B2 (D) was measured by MTT assay as described in Fig. 3. * significant *versus* doxorubicin treatment alone ($P < 0.05$).

with previous studies of 1,4-DHPs (Foroughinia et al., 2008; Mehdipour et al., 2007). Also there was no relationship between alkyl chain size (R_1) and CCB activity.

The cytotoxicity results of 1,4-DHPs studied in this project as well as our previous observations (Firuzi et al., 2013; Foroughinia et al., 2008) indicate that the anticancer effect is highly dependent on the substituent at the C_4 position. The presence of 1-methyl-5-nitro-imidazole-2-yl moiety at this position considerably lowers the cytotoxic effect, while nitrophenyl moiety seems to boost the activity. In addition, asymmetrical molecules are much better cytotoxic agents compared to symmetrical DHPs (Firuzi et al., 2013; Foroughinia et al., 2008; Mehdipour et al., 2007).

P-gp transporter inhibition and the resultant MDR reversal effect of the synthesized DHPs was evaluated by Rh123 efflux and MTT reduction assays in MES-SA/DX5 cells. Results of Rh123 efflux assay indicated that most of DHP compounds, especially those bearing nitrophenyl at C_4 position (A1B1 to A4B3), significantly decreased Rh123 efflux compared to control and had a dose dependent P-gp inhibitory effect. Therefore, it appears that alterations of the substituent at C_4 position have also considerable effects on the P-gp inhibitory activity. Although the presence of longer alkyls at C_5 improved P-gp inhibition (except for A4B1, A3B2 and A4B3), the aromatic ring at C_4 position seems to be a more important factor influencing Rh123 efflux inhibition.

Also based on the results obtained from the alteration of doxorubicin's IC_{50} value in MES-SA/DX5 cells, DHPs with nitrophenyl at C_4 position had higher activities compared to those with hetero aromatic moieties at this position (A1B4 to A3B5). On the other hand, synthesized DHPs did not increase cytotoxicity of doxorubicin on non-resistant MES-SA cells, which rules out a non-specific synergistic effect of these derivatives with doxorubicin.

The findings on the alteration of doxorubicin's IC_{50} in MES-SA/DX5 cells generally confirmed the results of Rh123 reflux. In both methods, replacement of nitrophenyl with hetero aromatic moieties at C_4 (as in A1B4 to A3B5) leads to a reduction of MDR reversal activity. Further, DHPs with 2-nitrophenyl as aromatic ring were weaker than those with 3 or 4-nitrophenyl at C_4 position. The compound A2B2 could not be properly evaluated for MDR reversal effect on MES-SA/DX5 cells by MTT assay at concentrations higher than 1 μM, because it had a high cytotoxicity on these cells, which would have been confounded with MDR reversal effect.

In conclusion, DHPs seem to provide a promising scaffold for the discovery of P-gp modulators and cytotoxic agents and SAR studies should be performed to determine the important structural features required for higher activity and lower potential side effects. Compounds A2B2 and A3B2 (bearing 3-nitrophenyl at C_4 position) showed the strongest P-gp inhibitory activity in Rh123 efflux assay, therefore, it appears that the presence of 3-nitrophenyl ring at C_4 position increases the P-gp mediated MDR reversal activity. While CCB activity of A3B2 did not differ from that of nifedipine, compound A2B2 was the most promising agent, as it was the most potent P-gp inhibitor, had a high direct anticancer activity against 4 cancer cells (IC_{50} range: 3.77–

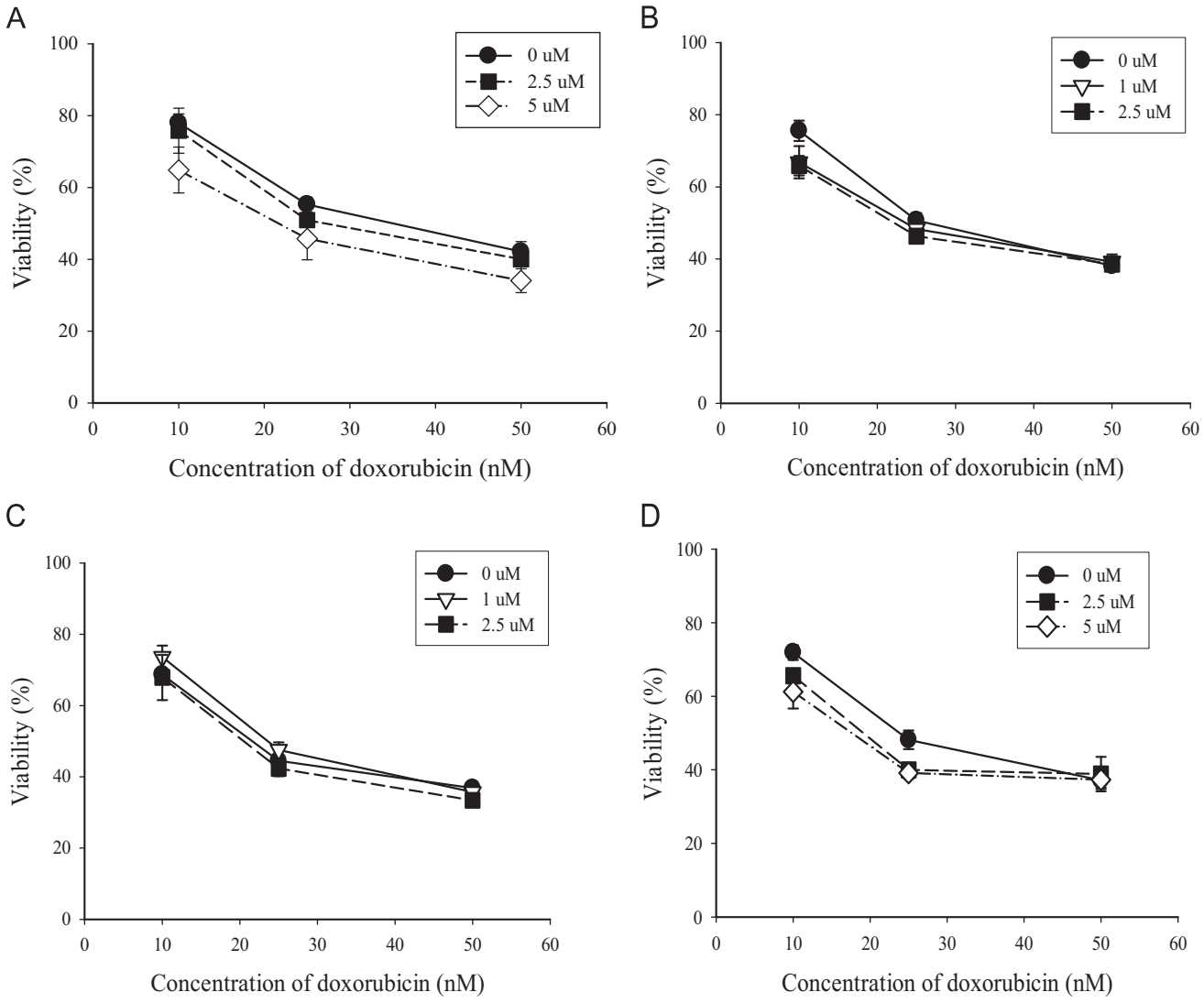

Fig. 5. Effect of synthesized derivatives on the response to doxorubicin in MES-SA cells. Effect of doxorubicin on the viability of MES-SA (non-resistant) cells in the absence or presence of the most potent MDR reversal compounds A2B1 (A), A3B1 (B), A4B1 (C) and A3B2 (D) was measured by MTT assay as described in Fig. 3.

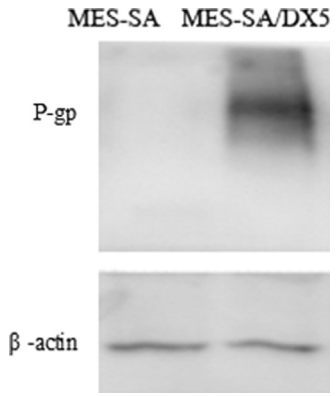

Fig. 6. P-gp expression in MES-SA/DX5 and MES-SA cell lines. Proteins were extracted from cells and loaded onto SDS polyacrylamide gel (7.5%) and analyzed for P-gp and β-actin expression using specific antibodies.

15.60 μM) and was also a weaker CCB agent compared to nifedipine. These findings are in agreement with the results of our previous study, which showed that the most active MDR reversal DHPs with high cytotoxicity, possessed 3-nitrophenyl ring and alkyl chain (ethyl and isopropyl) at C_4 and C_5 positions, respectively (Firuzi et al., 2013). On the other hand, compound A2B5 with 2-thienyl at C_4 position, showed the highest cytotoxicity (stronger than cisplatin) and low CCB properties but it had no MDR reversal effect. This compound could be suggested for further cytotoxic assessments.

Acknowledgments

The authors wish to thank the financial support of the Vice-Provost for Research, Shiraz University of Medical Sciences, Iran. The results reported in this paper were part of the Pharm.D. Thesis of Farnaz Shekari (Thesis Number: 447).

References

Carosati, E., Ioan, P., Micucci, M., Broccatelli, F., Cruciani, G., Zhorov, B.S., Chiarini, A., Budriesi, R., 2012. 1,4-Dihydropyridine scaffold in medicinal chemistry, the story so far and perspectives (part 2): action in other targets and antitargets. Curr. Med. Chem. 19, 4306–4323.

Coburger, C., Wollmann, J., Krug, M., Baumert, C., Seifert, M., Molnár, J., Lage, H., Hilgeroth, A., 2010. Novel structure–activity relationships and selectivity

profiling of cage dimeric 1, 4-dihydropyridines as multidrug resistance (MDR) modulators. Bioorg. Med. Chem. 18, 4983–4990.
Edraki, N., Mehdipour, A.R., Khoshneviszadeh, M., Miri, R., 2009. Dihydropyridines: evaluation of their current and future pharmacological applications. Drug Discov. Today 14, 1058–1066.
Firuzi, O., Javidnia, K., Mansourabadi, E., Saso, L., Mehdipour, A.R., Miri, R., 2013. Reversal of multidrug resistance in cancer cells by novel asymmetrical 1,4-dihydropyridines. Arch. Pharm. Res. 36, 1392–1402.
Foroughinia, F., Javidnia, K., Amirghofran, Z., Mehdipour, A., Miri, R., 2008. Design and synthesis of new symmetrical derivatives of dihydropyridine containing a pyridyl group on the 3, 5-positions and evaluation of their cytotoxic and multidrug resistance reversal activity. J. Pharm. Pharmacol. 60, 1481–1489.
Gottesman, M.M., 1993. How cancer-cells evade chemotherapy—16th Richard-and-Hinda-Rosenthal-Foundation Award Lecture. Cancer Res. 53, 747–754.
Hahn, K.A., Legendre, A.M., Schuller, H.M., 1997. Amputation and dexniguldipine as treatment for canine appendicular osteosarcoma. J. Cancer Res. Clin. Oncol. 123, 34–38.
Hilgeroth, A., Baumert, C., Coburger, C., Seifert, M., Krawczyk, S., Hempel, C., Neubauer, F., Krug, M., Molnár, J., Lage, H., 2013. Novel structurally varied N-Alkyl 1,4-dihydropyridines as ABCB1 inhibitors: structure-activity relationships, biological activity and first bioanalytical evaluation. Med. Chem. 9, 487–493.
Jassbi, A.R., Miri, R., Asadollahi, M., Javanmardi, N., Firuzi, O., 2014. Cytotoxic, antioxidant and antimicrobial effects of nine species of woundwort (Stachys) plants. Pharm. Biol. 52, 62–67.
Khoshneviszadeh, M., Edraki, N., Javidnia, K., Alborzi, A., Pourabbas, B., Mardaneh, J., Miri, R., 2009. Synthesis and biological evaluation of some new 1,4-dihydropyridines containing different ester substitute and diethyl carbamoyl group as anti-tubercular agents. Bioorg. Med. Chem. 17, 1579–1586.
Kumar, P., Kumar, A., Song, Z.-H., 2014. Structure–activity relationships of fatty acid amide ligands in activating and desensitizing G protein-coupled receptor 119. Eur. J. Pharmacol. 723, 465–472.
Laupeze, B., Amiot, L., Bertho, N., Grosset, J., Lehne, G., Fauchet, R., Fardel, O., 2001. Differential expression of the efflux pumps P-glycoprotein and multidrug resistance-associated protein in human monocyte-derived dendritic cells. Hum. Immunol. 62, 1073–1080.
Liscovitch, M., Lavie, Y., 2002. Cancer multidrug resistance: a review of recent drug discovery research. Investig. Drugs J. 5, 349–355.
Liu, F.S., 2009. Mechanisms of chemotherapeutic drug resistance in cancer therapy—a quick review. Taiwan. J. Obstet. Gynecol. 48, 239–244.
Mehdipour, A.R., Javidnia, K., Hemmateenejad, B., Amirghofran, Z., Miri, R., 2007. Dihydropyridine derivatives to overcome atypical multidrug resistance: design, synthesis, QSAR studies, and evaluation of their cytotoxic and pharmacological activities. Chem. Biol. Drug Des. 70, 337–346.
Memarian, H.R., Mirjafari, A., 2005. Solid state photochemistry of 1, 4-dihydropyridines. Bioorg. Med. Chem. Lett. 15, 3423–3425.
Miri, R., Javidnia, K., Mirkhani, H., Hemmateenejad, B., Sepeher, Z., Zalpour, M., Behzad, T., Khoshneviszadeh, M., Edraki, N., Mehdipour, A.R., 2007. Synthesis, QSAR and calcium channel modulator activity of new hexahydroquinoline derivatives containing nitroimidazole. Chem. Biol. Drug Des. 70, 329–336.
Moghadam, M., Nasr-Esfahani, M., Tangestaninejad, S., Mirkhani, V., 2006. Mild and efficient oxidation of Hantzsch 1,4-dihydropyridines with sodium periodate catalyzed by a new polystyrene-bound Mn(TPP)Cl. Bioorg. Med. Chem. Lett. 16, 2026–2030.
Morshed, S.R.M., Hashimoto, K., Murotani, Y., Kawase, M., Shaha, A., Satoh, K., Kikuchi, H., Nishikawa, H., Maki, J., Sakagami, H., 2005. Tumor-specific cytotoxicity of 3, 5-dibenzoyl-1, 4-dihydropyridines. Anticancer Res. 25, 2033–2038.
Mosmann, T., 1983. Rapid colorimetric assay for cellular growth and survival: application to proliferation and cytotoxicity assays. J. Immunol. Methods 65, 55–63.
Munić, V., Kelnerić, Ž., Mikac, L., Eraković Haber, V., 2010. Differences in assessment of macrolide interaction with human MDR1 (ABCB1, P-gp) using rhodamine-123 efflux, ATPase activity and cellular accumulation assays. Eur. J. Pharm. Sci. 41, 86–95.
Ozben, T., 2006. Mechanisms and strategies to overcome multiple drug resistance in cancer. FEBS Lett. 580, 2903–2909.
Palmeira, A., Vasconcelos, M.H., Paiva, A., Fernandes, M.X., Pinto, M., Sousa, E., 2012. Dual inhibitors of P-glycoprotein and tumor cell growth: (re)discovering thioxanthones. Biochem. Pharmacol. 83, 57–68.
Saini, A., Kumar, S., Sandhu, J.S., 2008. Hantzsch reaction: recent advances in Hantzsch 1,4-dihydropyridines. J. Sci. Ind. Res. 67, 95–111.
Sarkarzadeh, H., Miri, R., Firuzi, O., Amini, M., Razzaghi-Asl, N., Edraki, N., Shafiee, A., 2013. Synthesis and antiproliferative activity evaluation of imidazole-based indeno[1,2-b]quinoline-9,11-dione derivatives. Arch. Pharm. Res. 36, 436–447.
Sica, D.A., 2006. Pharmacotherapy review: calcium channel blockers. J. Clin. Hypertens. 8, 53–56.
Singhuber, J., Baburin, I., Ecker, G.F., Kopp, B., Hering, S.J., 2011. Insights into structure-activity relationship of GABAA receptor modulating coumarins and furanocoumarins. Eur. J. Pharmacol. 668, 57–64.
Tsuruo, T., Iida, H., Nojiri, M., Tsukagoshi, S., Sakurai, Y., 1983. Circumvention of vincristine and adriamycin resistance in vitro and in vivo by calcium influx blockers. Cancer Res. 43, 2905–2910.
Twentyman, P.R., Rhodes, T., Rayner, S., 1994. A comparison of rhodamine 123 accumulation and efflux in cells with P-glycoprotein-mediated and MRP-associated multidrug resistance phenotypes. Eur. J. Cancer 30, 1360–1369.
Viale, M., Cordazzo, C., De Totero, D., Budriesi, R., Rosano, C., Leoni, A., Ioan, P., Aiello, C., Croce, M., Andreani, A., Rambaldi, M., Russo, P., Chiarini, A., Spinelli, D., 2011. Inhibition of MDR1 activity and induction of apoptosis by analogues of nifedipine and diltiazem: an in vitro analysis. Investig. New Drugs 29, 98–109.
Voigt, B., Coburger, C., Monar, J., Hilgeroth, A., 2007. Structure-activity relationships of novel N-acyloxy-1,4-dihydropyridines as P-glycoprotein inhibitors. Bioorg. Med. Chem. 15, 5110–5113.
Wesolowska, O., Paprocka, M., Kozlak, J., Motohashi, N., Dus, D., Michalak, K., 2005. Human sarcoma cell lines MES-SA and MES-SA/Dx5 as a model for multidrug resistance modulators screening. Anticancer Res. 25, 383–389.
Xi, G.M., Sun, B., Jiang, H.H., Kong, F., Yuan, H.Q., Lou, H.X., 2010. Bisbibenzyl derivatives sensitize vincristine-resistant KB/VCR cells to chemotherapeutic agents by retarding P-gp activity. Bioorg. Med. Chem. 18, 6725–6733.
Yamakage, M., Namiki, A., 2002. Calcium channels-basic aspects of their structure, function and gene encoding; anesthetic action on the channels—a review. Can. J. Anesth. 49, 151–164.
Zarrin, A., Mehdipour, A.R., Miri, R., 2010. Dihydropyridines and multidrug resistance: previous attempts, present state, and future trends. Chem. Biol. Drug Des. 76, 369–381.